Limits on Spin-Dependent WIMP-Nucleon Interactions from the Cryogenic Dark Matter Search

Jeffrey P. Filippini, for the CDMS Collaboration
Department of Physics, University of California, Berkeley, CA 94720, USA

We give a brief introduction to the physics of spin-dependent WIMP interactions and report the results of an analysis of recent data sets from the Cryogenic Dark Matter Search (CDMS) in terms of spin-dependent WIMP-nucleon interactions on ^{73}Ge and ^{29}Si. The primary data are from the first run of CDMS at the Soudan Underground Laboratory, and data from a prior run at the Stanford Underground Facility (6.6 raw kg-day Si exposure at 20 mwe) are used to extend our reach in the case of low WIMP mass. These data exclude new regions of spin-dependent WIMP-nucleon interaction parameter space. The parameter space explored is relevant to spin-dependent interpretations of the annual modulation signal reported by the DAMA experiment, but does not yet probe preferred regions of supergravity parameter space.

1. Introduction

Determining the nature of the dark matter which dominates the evolution of structure in our universe is one of the most pressing questions of modern cosmology. The most promising class of candidates for this dark matter is weakly interacting massive particles (WIMPs) [1], in particular the lightest neutralino in supersymmetric (SUSY) extensions to the Standard Model [2]. In recent years, numerous experimental groups have sought to detect WIMPs directly via their elastic scattering off atomic nuclei in a target mass [3].

In the extreme nonrelativistic limit, the nucleon coupling of any WIMP is characterized by two distinct terms: scalar and axial vector [4]. The former leads to an interaction amplitude dependent on the numbers of WIMPs and nucleons present, known as "spin-independent" coupling. The latter gives an amplitude dependent on the scalar product of the WIMP and nucleon spins, known as "spin-dependent" coupling. For the purposes of direct detection, a WIMP candidate may thus be characterized by five quantities: its mass (M_χ), its spin-independent couplings to the proton and neutron (f_p, f_n), and its spin-dependent couplings to these nucleons (a_p, a_n). In order to compute an event rate, it is also necessary to assume some phase space distribution for the WIMPs comprising the galactic halo, e.g. the "standard halo model" [5].

The expected direct detection signal of SUSY neutralinos are generally dominated by their spin-independent couplings. The various WIMP-nucleon scattering amplitudes add coherently across the nucleus (with corrections for finite-momentum-transfer effects using a form factor $F^2(q)$) to give a total WIMP-nucleus elastic scattering cross section

$$\frac{d\sigma^{SI}_{\chi N}}{dq^2} = \frac{1}{\pi v^2}[Zf_p + (A-Z)f_n]^2 F^2(q),$$

where v is the incident WIMP velocity, q is the momentum transferred, Z is the atomic number of the target nucleus, and A is its mass number. Neutralino-nucleon interaction processes (usually dominated by Higgs exchange) are expected to give $f_p \approx f_n$ [2], yielding $\sigma^{SI}_A \sim f_p^2 A^2$. This A^2 factor may be very large (e.g. ~ 5000 for Ge), leading scalar interactions to dominate detection event rates for experiments using heavy target nuclides. Such experiments quote model-independent results in terms of a single limit curve (or allowed region) in the $\sigma^{SI}_p - M_\chi$ plane.

In contrast, the total spin-dependent scattering amplitude on a pair of nucleons with opposite spin is negligible for low momentum transfers, leaving the scattering amplitude determined roughly by the spins of the *unpaired* nucleons in a given nucleus. Sensitivity to such interactions thus demands the use of target nuclides with unpaired neutrons or protons. The general form of the differential cross section for WIMP-nucleus elastic scattering, valid at any momentum transfer q, is [6]

$$\frac{d\sigma^{SD}_{\chi N}}{dq^2} = \frac{8G_F^2}{(2J+1)v^2} S(q), \qquad (1)$$

where J is the nuclear spin, G_F is Fermi's constant, and

$$S(q) = a_0^2 S_{00}(q) + a_0 a_1 S_{01}(q) + a_1^2 S_{11}(q), \qquad (2)$$

with $a_0 = a_p + a_n$ and $a_1 = a_p - a_n$. In SUSY neutralino models, neutralino-nucleon cross spin-dependent couplings, given primarily by Z^0 and squark exchange, are generally several orders of magnitude *larger* than in the spin-independent case [7], but usually fail to dominate direct detection event rates because they do not benefit from A^2 scaling. Nonetheless, such interactions may become important if the spin-independent coupling is strongly suppressed (i.e. for a pure gaugino WIMP [2]), and can often provide a lower limit to the WIMP-nucleus elastic cross section by dominating the scattering amplitude in less-detectable regions of parameter space [8]. In general, consideration of such couplings when interpreting experimental results more fully constrains WIMP parameter space and allows exploration of alternate interpretations of possible signals [9, 10].

Figure 1: A CDMS II ZIP (Z-sensitive Ionization and Phonon) detector and its housing. Data for this analysis were taken with a single "tower" of six such detectors.

2. Data Sets

The Cryogenic Dark Matter Search (CDMS) [11, 12] is an experiment designed to search for WIMPs via their interaction with nuclei in semiconductor crystals at millikelvin temperatures. CDMS utilizes ZIP detector technology (see Figure 1) [13] to discriminate between electron recoils (most backgrounds) and nuclear recoils (WIMPs and neutrons) on an event-by-event basis via a simultaneous measurement of ionization and athermal phonons. Under the assumptions of the standard halo model, CDMS currently sets the lowest limit on spin-independent WIMP interactions.

The CDMS detectors are made of natural Ge and Si. Both materials are composed predominantly of spinless isotopes with negligible sensitivity to spin-dependent WIMP interactions. Each does, however, contain one isotope with non-zero nuclear spin in significant proportion: ^{73}Ge (spin-9/2) makes up 7.73% of natural Ge, while ^{29}Si (spin-1/2) comprises 4.68% of natural Si. Each isotope contains a single unpaired neutron, making CDMS sensitive primarily to spin-dependent interactions with atomic neutrons (a_n) rather than protons (a_p).

The analysis presented here is based on two CDMS II data runs using the first "tower" of six ZIP detectors. The primary data set was taken between October 11, 2003 and January 11, 2004 at the Soudan Underground Laboratory in northern Minnesota. This run accumulated 52.6 raw (before cuts) kg-days of Ge exposure (5.3 raw kg-days Si exposure), and is described in detail in [11, 14]. Due to the conservative analysis thresholds used in this run (10 keV for 3 Ge ZIPs, 20 keV for Si ZIPs and 1 Ge ZIP), we have also incorporated data from a run of the same detectors at the shallow Stanford Underground Facility between December 2001 and April 2002, described in detail in [15]. This run collected 65.8 raw kg-days of Ge exposure (6.6 raw kg-days Si) with substantially lower thresholds (5 keV on all detectors except 20 keV on one Ge ZIP), but due to its limited rock overburden a number of events (presumably muon-induced neutrons) were observed. The former run found no signal events in the initial blind analysis and one event in the subsequent non-blind analysis. The latter found 20 Ge and 2 Si single-scatter nuclear recoil events in the signal region, consistent with the expected neutron background.

The data, cuts, and resulting event counts used here are identical to those from the original references. In the case of the first Soudan run, we choose to plot results from the second, non-blind analysis (blind analysis curves are essentially identical). The Si data from this analysis has not previously been published. Scaling the raw exposures down by the isotopic abundances above, we obtain 4.1 raw kg-days ^{73}Ge (0.25 raw kg-days ^{29}Si) exposure at the deep site and 5.1 raw kg-days ^{73}Ge (0.31 raw kg-days ^{29}Si) at the shallow site.

3. Model-independent Analysis Framework

It is significantly more complex to compute a model-independent result in the case of spin-dependent WIMP interactions than in the spin-independent case. Spin structure varies substantially between nuclear species and demands detailed nuclear modeling. Further, the WIMP-proton and WIMP-neutron couplings are not necessarily equal [16] (though they are often of similar magnitude in models of interest [17]). In this section we review a model-independent framework due to Tovey et al. [16] and expanded upon by [10, 18] for the interpretation of experimental results in terms of spin-dependent interactions. From here on, we make the assumption that $f_p = f_n = 0$ (pure spin-dependent coupling).

3.1. Spin Structure

The "spin structure function" $S(q)$ encompasses the magnitude of the spin associated with the protons and neutrons of the desired nucleus (often quoted as the proton and neutron spin expectation values in the limit of vanishing momentum transfer, $\langle S_p \rangle$ and $\langle S_n \rangle$), as well as the momentum-transfer effects of the spatial distribution of that spin. The function $S(q)$ is clearly WIMP model-dependent, with its form determined by the ratio a_p/a_n and its magnitude by $a_p^2+a_n^2$. In the absence of direct measurements, the spin structure function must be determined separately for each nuclide using a nuclear structure model.

For ^{29}Si, the major efforts at computing nuclear spin structure have been via large-basis shell model

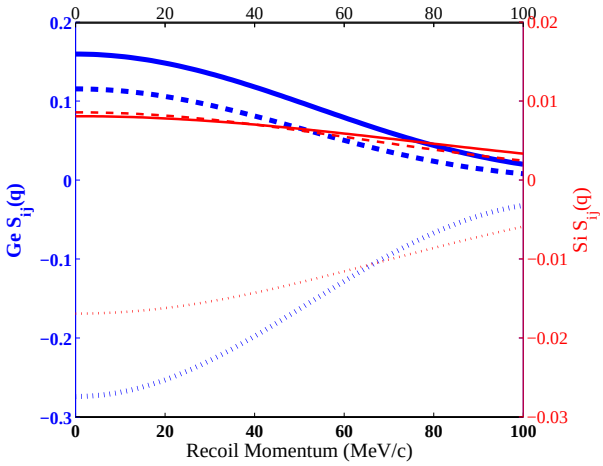

Figure 2: Spin-dependent structure functions $S_{00}(q)$ (solid), $S_{11}(q)$ (dashed), and $S_{01}(q)$ (dotted) used in this analysis. The Ge structure functions (dark, bold) are taken from [19], while the Si functions (light, thin) are taken from [20].

simulations by Ressell et al. [20] and Divari et al. [21]. The results of both calculations agree in the zero-momentum transfer limit within their reported precisions ($\langle S_p \rangle = 0.002$, $\langle S_n \rangle = 0.13$), and both reproduce the experimental magnetic moment ($\mu = -0.555\mu_N$) to within 10% without explicit rescaling ("quenching"). We use the results of Ressell et al. in this analysis.

The most complete shell model studies of ^{73}Ge to date have been carried out by Ressell et al. [20] and Dimitrov et al. [19]. The former result requires "quenching" to bring its predicted value of the nuclear magnetic moment ($\mu = -1.239\mu_N$ before quenching) in line with experiment ($\mu = -0.879\mu_N$), while the "hybrid model" used in the latter does not ($\mu = -0.920\mu_N$). Both models give zero-momentum transfer values of $\langle S_n \rangle$ within $\sim 2\%$ of one another, but their values for $\langle S_p \rangle$ differ by a factor of 3. We follow the results of Dimitrov et al., and these structure functions are illustrated in Figure 2.

3.2. Plotting Conventions

For easy comparisons between experiments, we follow Tovey et al. and report two two-dimensional allowed regions for each experiment: one in the case $a_n = 0$ (pure proton coupling), one in the case $a_p = 0$ (pure neutron coupling). For this purpose, we define standard WIMP-nucleon cross sections

$$\sigma^{SD}_{p,n} = \frac{8(J+1)}{\pi J} G_F^2 \mu^2_{\chi p,n} a^2_{p,n}, \qquad (3)$$

where $\mu_{\chi p,n}$ is the WIMP-nucleon reduced mass. In each case, we use the spin structure function $S(q)$ appropriate to the the assumed couplings. Each experiment thus determines allowed regions in two $\sigma^{SD} - M_\chi$ planes, allowing for easy comparison.

In order to explore more generic models in which a_p and a_n are both non-zero, we plot directly the allowed region of the $a_p - a_n$ plane for various choices of WIMP mass M_χ. This framework has been described by Giuliani [18] in the limit of vanishing momentum transfer and generalized by Savage et al. [10]. Null experimental results yield elliptical allowed regions in this formalism, while signal observations correspond to elliptical "rings". The orientation of each ellipse is determined by the given experiment's choice of target material, and so combining results from multiple target materials can substantially restrict the allowed region.

4. Limits on WIMP Parameters

4.1. Pure Neutron or Proton Couplings

In Figure 3 we plot upper-limit contours in the $M_\chi - \sigma^{SD}$ plane in the limiting cases of pure neutron coupling ($a_p = 0$) and pure proton coupling ($a_n = 0$) for the CDMS data sets described above. All CDMS curves are computed using Yellin's Optimum Interval method [25]. The resulting Ge limit is comparable to that estimated in [10], but our use of experimentally-determined efficiencies makes the current limit somewhat stronger ($\sim 20\%$ near 50 GeV/c^2). For comparison, we also plot interpretations from [10] of the DAMA annual modulation signal [9]. Further comparison with other experiments and with theory are given in Figure 5. Combined, the various CDMS data runs exclude new regions of parameter space for pure WIMP-neutron spin-dependent couplings. These data are inconsistent with an interpretation of the DAMA signal in terms of such interactions within the standard halo model.

In the case of purely proton-coupled WIMPs, the lack of unpaired protons in its nuclides limits the sensitivity of CDMS. Contributions from nuclear excitations with non-zero $\langle S_p \rangle$, however, give ^{73}Ge a non-vanishing sensitivity to such couplings. CDMS has begun to explore the regions of pure WIMP-proton parameter space associated with the DAMA annual modulation signal, and will explore substantially more by the end of CDMS II's run.

4.2. General Limits on Parameter Space

CDMS's limits can also be expressed in the $a_p - a_n$ plane for various choices of WIMP mass. Two such choices (13 GeV/c^2 and 50 GeV/c^2) are shown in Figure 4. Again, limit contours are determined using the Optimum Interval method. The left plot illustrates

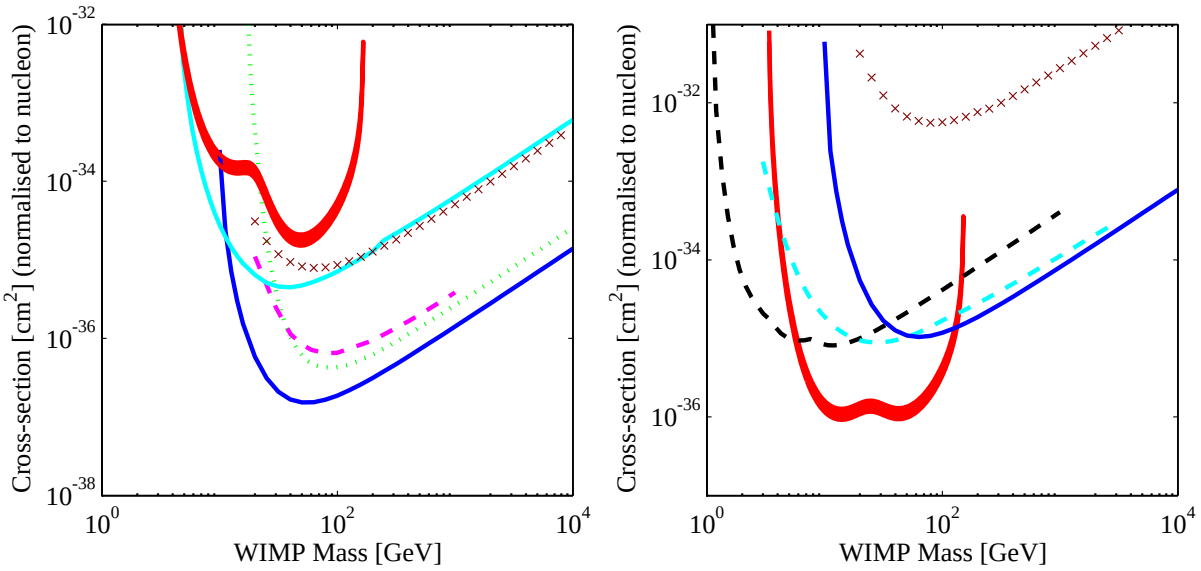

Figure 3: 90% confidence level contours for recent data sets from CDMS and other experiments, plotted in the cases of (*left*) pure neutron and (*right*) pure proton coupling. The region above each limit curve is excluded by the corresponding experimental data set. The CDMS limit curves are, respectively, Stanford Si (light solid), Soudan Si (crosses), and Soudan Ge (dark solid). As benchmarks, we also include interpretations of the DAMA annual modulation signal (filled regions), as computed in [10]. Other experimental curves are: *left* Edelweiss [22] (dashed) and DAMA/Xe (as computed in [10]) (dotted); *right* CRESST I (as computed in [10]) (dark dashed) and SIMPLE [23](light dashed). Plots made with [24].

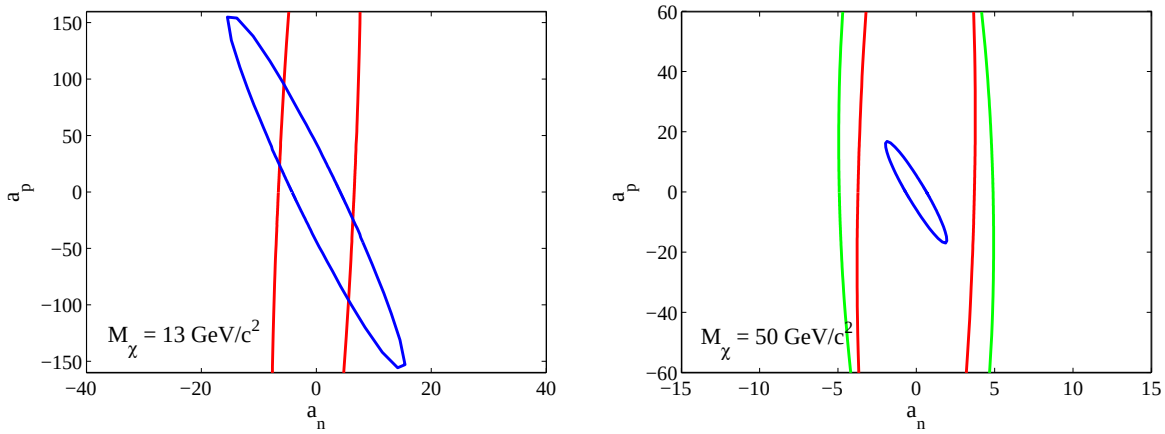

Figure 4: Regions in the $a_p - a_n$ plane allowed (at the 90% confidence level) by analyses of various CDMS data sets. Each analysis excludes the exterior of the corresponding ellipse. Two choices of WIMP mass M_χ are shown: 13 GeV/c^2 (*left*) and 50 GeV/c^2 (*right*). Counting inward on the plot at right, the ellipses represent limits due to CDMS Stanford Si, CDMS Soudan Si, and CDMS Soudan Ge. The limits at left are due to CDMS Stanford Si (larger) and CDMS Soudan Ge (smaller). Due to the 20 keV analysis threshold in the Soudan Si data set, no limit can be set using that data set within the standard halo model for WIMP masses below $\sim$ 20 GeV/c^2.

the advantage of using two active isotopes: the region allowed by both nuclides (approximately the overlap of the two ellipses) may be significantly smaller than either ellipse individually. In the case of CDMS, ^{73}Ge provides the best overall sensitivity, but the generally weaker constraint from ^{29}Si gives further constraint at low masses. In particular, the long "ends" of both ellipses are cut off. The lengths of these ellipses are based on near-cancellations in the spin-dependent structure functions, and so are expected to have substantial uncertainties.

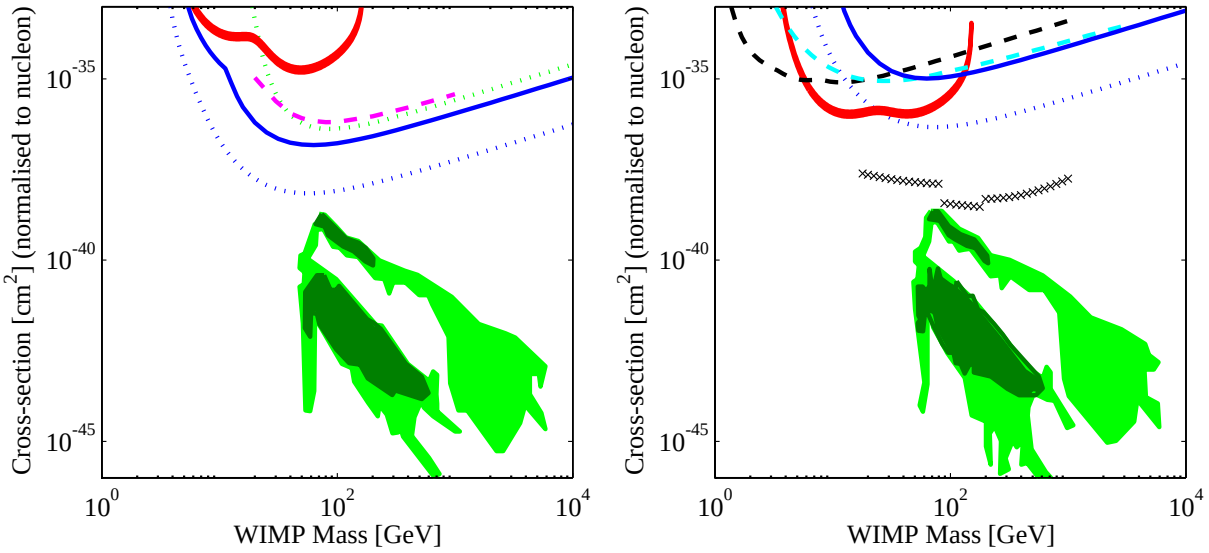

Figure 5: Limits (90% confidence level) on spin-dependent WIMP-nucleon interactions in the case of (*left*) pure neutron and (*right*) pure proton coupling. The envelopes of the lowest CDMS curves in Figure 3 are shown as solid lines. Allowed regions from other major experiments are as shown in Figure 3, with the addition of the results of Super-Kamiokande's indirect search [26] in terms of spin-dependent proton interactions (crosses). In both plots, upper filled regions represent the DAMA/NaI signal region and lower filled regions are allowed regions from mSUGRA models [27], both with (dark filled) and without (light filled) a 1σ g-2 constraint. The lower dotted lines represents the expected reach of CDMS II at Soudan.

4.3. Supersymmetric Dark Matter

Spin-dependent couplings are generally less promising in the context of direct detection of supersymmetric dark matter. Scans of mSUGRA parameter space suggest [7] that event rates due to spin-independent interactions exceed those due to spin-dependent interactions in models with all but the lowest cross sections. In Figure 5 we compare the CDMS limit curves in Figure 3 with the results of Markov Chain Monte Carlo scans of WMAP-allowed mSUGRA parameter space by Baltz and Gondolo [27, 28]. CDMS II is not expected to explore the parameter space of such models. An increase in exposure by at least two orders of magnitude is required, which may be possible with larger-scale implementations of similar detector technology (e.g. the proposed SuperCDMS [29]).

5. Conclusions and Future Prospects

Due to its large exposure and excellent background discrimination, CDMS possesses a substantial sensitivity to spin-dependent WIMP-nucleon interactions, despite the predominantly spinless nature of its target materials. This sensitivity is competitive with that of other major experiments, and in particular its limit is among the best yet published under the assumptions of pure neutron coupling and a standard galactic halo. Such limits also further constrain possible interpretations of the DAMA annual modulation signal.

In the upcoming months, our collaboration will acquire and analyze two substantially larger data sets that will extend our reach by a factor of ≈ 20. We are currently analyzing data from a run with 12 ZIP detectors at Soudan in 2004, and we will shortly begin a run with our full complement of 30 ZIPs. These data will allow us to explore far deeper into spin-independent and spin-dependent WIMP parameter space.

Acknowledgments

The authors thank C. Savage for useful discussions and E. Baltz for data on theoretical predictions. This work is supported by the National Science Foundation under Grant No. PHY-9722414, by the Department of Energy under contracts DE-AC03-76SF00098, DE-FG03-90ER40569, DE-FG03-91ER40618, and by Fermilab, operated by the Universities Research Association, Inc., under Contract No. DE-AC02-76CH03000 with the Department of Energy. JF is supported by an NDSEG Fellowship from the Army Research Office. The ZIP detectors were fabricated in the Stanford Nanofabrication Facility operated under NSF.

References

[1] B. W. Lee and S. Weinberg, Phys. Rev. Lett. **39**, 165 (1977).

[2] G. Jungman, M. Kamionkowski and K. Griest, Phys. Rept. **267**, 195 (1996) [arXiv:hep-ph/9506380].

[3] R. J. Gaitskell, Ann. Rev. Nuc. Part. Sci. **54**, 315 (2004).

[4] A. Kurylov and M. Kamionkowski, Phys. Rev. D **69**, 063503 (2004) [arXiv:hep-ph/0307185].

[5] J. D. Lewin and P. F. Smith, Astropart. Phys. **6**, 87 (1996).

[6] J. Engel, Phys. Lett. B **264**, 114 (1991).

[7] V. A. Bednyakov and H. V. Klapdor-Kleingrothaus, Phys. Rev. D **63**, 095005 (2001) [arXiv:hep-ph/0011233].

[8] V. A. Bednyakov, F. Simkovic and I. V. Titkova, arXiv:hep-ph/0412067.

[9] R. Bernabei *et al.*, Riv. Nuovo Cim. **26N1**, 1 (2003) [arXiv:astro-ph/0307403].

[10] C. Savage, P. Gondolo and K. Freese, Phys. Rev. D **70**, 123513 (2004) [arXiv:astro-ph/0408346].

[11] D. S. Akerib *et al.* [CDMS Collaboration], Phys. Rev. Lett. **93**, 211301 (2004) [arXiv:astro-ph/0405033].

[12] R. W. Ogburn *et al.*, *these proceedings* (2005).

[13] K. D. Irwin, Ph.D. thesis, Stanford University (1995).

[14] D. S. Akerib *et al.* [CDMS collaboration], in preparation.

[15] D. S. Akerib *et al.* [CDMS Collaboration], Phys. Rev. D **68**, 082002 (2003) [arXiv:hep-ex/0306001].

[16] D. R. Tovey, R. J. Gaitskell, P. Gondolo, Y. Ramachers and L. Roszkowski, Phys. Lett. B **488**, 17 (2000) [arXiv:hep-ph/0005041].

[17] V. A. Bednyakov, Phys. Atom. Nucl. **67**, 1931 (2004) [Yad. Fiz. **67**, 1957 (2004)] [arXiv:hep-ph/0310041].

[18] F. Giuliani, Phys. Rev. Lett. **93**, 161301 (2004).

[19] V. Dimitrov, J. Engel and S. Pittel, Phys. Rev. D **51**, 291 (1995) [arXiv:hep-ph/9408246].

[20] M. T. Ressell, M. B. Aufderheide, S. D. Bloom, K. Griest, G. J. Mathews and D. A. Resler, Phys. Rev. D **48**, 5519 (1993).

[21] P. C. Divari, T. S. Kosmas, J. D. Vergados and L. D. Skouras, Phys. Rev. C **61**, 054612 (2000).

[22] A. Benoit *et al.* [EDELWEISS Collaboration], arXiv:astro-ph/0412061.

[23] F. Giuliani and T. A. Girard, Phys. Lett. B **588**, 151 (2004) [arXiv:astro-ph/0311589].

[24] R. J. Gaitskell and V. Mandic, URL http://dmtools.berkeley.edu/limitplots/.

[25] S. Yellin, Phys. Rev. D **66**, 032005 (2002) [arXiv:physics/0203002].

[26] S. Desai *et al.* [Super-Kamiokande Collaboration], Phys. Rev. D **70**, 083523 (2004) [arXiv:hep-ex/0404025].

[27] E. A. Baltz, personal communication (2004).

[28] E. A. Baltz and P. Gondolo, JHEP **0410**, 052 (2004) [arXiv:hep-ph/0407039].

[29] P. Brink *et al.*, *these proceedings* (2005).